USGS-OFR-82-200A

UNITED STATES DEPARTMENT OF THE INTERIOR
GEOLOGICAL SURVEY

USGS-OFR--82-200A

DE84 900476

GEOLOGIC SETTING OF MASSIVE SULFIDE DEPOSITS AND HYDROTHERMAL VENTS ALONG THE SOUTHERN JUAN DE FUCA RIDGE

by

William R. Normark and Janet L. Morton
U.S. Geological Survey
Menlo Park, California

and

John R. Delaney
University of Washington
Seattle, Washington

Open-File Report 82-200A

This report is preliminary and has not been reviewed for conformity with U.S. Geological Survey editorial standards. Any use of trade names is for descriptive purposes only and does not imply endorsement by the USGS.

DISCLAIMER

GEOLOGIC SETTING OF MASSIVE SULFIDE DEPOSITS AND HYDROTHERMAL VENTS ALONG THE SOUTHERN JUAN DE FUCA RIDGE

by

W. R. Normark[1], J. L. Morton[1], and J. R. Delaney[2]

Since 1978, detailed photographic and submersible studies of the oceanic spreading ridge system in the eastern Pacific Ocean have identified polymetallic sulfide deposits and associated submarine hydrothermal springs at six locations between latitude 20°S on the East Pacific Rise and the Juan de Fuca Ridge west of Oregon (Fig. 1, Corliss and others, 1979; RISE Project Group, 1980; Hekinian and others, 1980; CYAMEX Scientific Team, 1981; Lonsdale and others, in press; Ballard and others, 1981; Hekinian and others, 1981). Four of these discoveries, including the one reviewed in this report, came in the last 18 months, and all of the deposits are located along the axes of ridges with medium or fast spreading rates. Lonsdale (1977) defines a medium spreading rate to include plate separation at 5 to 9 cm/yr; rates greater than 9 cm/yr represent fast spreading. Massive sulfide deposits have not been found along slow-spreading (<5 cm/yr) ridges, such as the Mid-Atlantic Ridge.

The Juan de Fuca Ridge is a medium-rate spreading axis with a total opening rate near 6 cm/yr that lies off the Pacific Northwest (Fig. 2). In 1979, we selected the southern segment of the Juan de Fuca Ridge as the initial survey area for the developing U.S. Geological Survey program on sulfide metallogenesis because:

(1) the spreading rate is nearly identical to those at then known areas of active hydrothermal vents along the East Pacific Rise near latitude 21°N and the Galapagos Rift near longitude 86°W;

(2) the magnetic-anomaly map (National Ocean Survey, 1974) and available detailed bathymetric data (Geological Survey of Canada and U.S. Geological Survey) show that the ridge segment north of the Blanco fracture zone is an area of relatively uniform spreading history and is tectonically uncomplicated. To the north of the area selected, hot-spot volcanism near the ridge axis has produced a chain of seamounts that complicates the ridge morphology. The Gorda Ridge, south of the Blanco fracture zone, has the same spreading rate but has a morphology similar to slow spreading ridges, with an axial valley floor about one kilometer deeper than the southern Juan de Fuca Ridge.

[1] U.S. Geological Survey, Menlo Park, California

[2] University of Washington, Seattle, Washington

Before the initial U.S.G.S. expedition to the study area in the fall of 1980, a reconnaissance survey of the entire Juan de Fuca Ridge system by University of Washington researchers (Delaney and others, 1981) showed that the axial valley floor of the selected ridge segment is underlain by fresh, glassy basalt indicating recent volcanic activity. At both the East Pacific Rise and Galapagos areas, hydrothermal activity is generally associated with the areas of youngest volcanic rocks along the axis (Ballard and others, 1981; Ballard and others, 1982). The only camera station along the southern Juan de Fuca Ridge (Delaney and others, 1981) provided several frames with benthic siphonophores similar in appearance to those seen at low temperature vents in the Galapagos area (Galapagos Biology Expedition Participants, 1979).

This report incorporates data from two cruises of the U.S.G.S. vessel S.P. LEE: (1) L12-80-WF from 29 October to 13 November 1980, and (2) L11-81-WF from 4 to 15 September 1981. The 1980 cruise occurred long after the optimum weather window for this region. The natural result was that no photographic or sample stations could be attempted during nearly continuous gale- and storm-force winds, which twice forced the vessel to depart the work area for safety. A detailed bathymetric survey of a 35-km segment of the ridge axial zone was completed nonetheless, and the bathymetric map compiled from this survey was used as the base for our second cruise in 1981. The second visit to the area was blessed with fair weather, and most of the cruise effort was devoted to photography and sampling, including dredging and hydrocasts in the axial valley segment shown in Figure 3, which is the central part of the area surveyed in 1980.

METHODS

Navigation

During the 1980 cruise when only bathymetric surveying was possible, an integrated navigation system combining satellite, LORAN C, and doppler-sonar data provided continuous position information for the S.P. LEE. In 1981, the integrated navigation system was supplemented by an acoustic transponder system to provide ship positions for all station work and to provide more accurate relative positions for mapping the shape of the axial valley floor. Up to four acoustic transponders provided range data for each position. The transponders are anchored on the inner valley walls above terraces on either side of the valley floor (B-B', Fig. 4); the units were floated 100 m above the seafloor, and this provided excellent position control over the valley floor. The summed horizontal range error for three-transponder fixes was generally less than 20 m. The position control was good enough to allow reoccupation of vent locations only 20 to 50 m in width.

The acoustic-transponder system provided position data for the photographic and sampling stations as well. During photographic stations, a relay transponder is placed 100 m above the camera frame. A pinger placed in the camera sled provides a record of the altitude of the camera (generally maintained at 4 to 6 m above the seafloor). This altitude data, together with the acoustically-determined slant range between the ship and relay transponder and the transponder-detemined positions for the ship and relay, allows direct calculation of the water depth at the times of each position, which were at 5-minute intervals for most of the station work.

Station Instruments

About half of the station time during the 1981 cruise was devoted to photography. Twelve stations were occupied (Figure 5) using a camera system developed at the University of Washington and loaned to us for the cruise. Two 35 mm cameras with 30-m rolls of film are operated serially, thus providing approximately 4-1/2 hours of bottom photographs every lowering (approximately 900 photographs per station). High-speed black-and-white film was used at all but one of the stations (#24) and was developed on board; station 24 was our only chance to obtain color photographs of a vent area previously identified with black-and-white film.

Thirteen dredge stations were attempted along the axial valley floor and inner walls. We used a round-frame chain-bag dredge on loan from the University of Washington. With the exception of the early dredge stations (3 and 4, Fig. 6) that were taken using a time-depth recorder, a 12-kHz pinger was attached to the dredge wire 200 m or 350 m above the dredge. The pinger record allowed us to dredge with a short wire scope, so that most dredge stations were only several hundred meters in length. During stations selected to recover sulfide deposits at vent areas, a relay transponder and pinger are attached at about 200 m above the dredge. The dredge is maintained just above the seafloor until the relay transponder shows the dredge adjacent to the vent. The dredge is then quickly lowered to the seafloor, dragged across the vent area, and then hauled clear of the bottom.

Two hydrocast stations along the axis utilized six 30-liter Niskin bottles placed at 50 m intervals between 1950 m and 2200 m depth (in water depths slightly greater than 2210 m). A 400-kg weightstand at the end of the wire was held just above the seafloor by monitoring the record from a 12-kHz pinger mounted 6 m above the weightstand. For both hydrocasts, ship position was maintained during the station using transponder navigation; and for station 25, a relay transponder was mounted below the lowest Niskin sampler to monitor the bottle position relative to a sulfide deposit (Fig. 6). Upon recovery of the bottles, separate samples were drawn off for measurement of the amount of helium-3, methane, and manganese in the water. From the remainder, 10 liters of untreated water were then drawn into plastic containers, sealed, and stored at 4°C; this water is still available.

RESULTS

Bathymetry

The November 1980 survey using 3.5-kHz and 12-kHz sounders provided a bathymetric map with a 25-m contour interval over an area 35 km along strike and 20 km in width. The southern Juan de Fuca Ridge is characterized by a relatively straight, symmetric 80-to-100-m-deep axial valley with no lateral offsets. The axial valley floor is about one kilometer wide and remarkably smooth. The depth of the valley floor changes gradually along strike, and near latitude 41°38'N the valley floor reaches its shallowest point within the mapped area (A-A', Fig. 4). The ridge segment centered about this high point on the longitudinal profile (area of Figure 3) was selected for the photographic and sampling study because hydrothermal activity at both the East

Pacific Rise 21°N site and the Galapagos Rift are found near local highs in the longitudinal profiles of these spreading centers.

The 1981 cruise also provided bathymetric data within the axial valley. The transponder-positioned profiles allowed us to refine the plan of the valley floor, and this new data was merged with the 1980 bathymetry to produce the map of the work area (Fig. 3). The valley floor has a gentle camber across strike, with the center of the valley being a few meters higher than the floor near the valley walls. A narrow depression along the center of the valley is nearly continuous except in the southern 3 kilometers of the study area. The width of the depression varies from about 50 m to 200 m, and the depths range from a few to about 25 m (Fig. 7).

Station work

Twelve camera stations, two hydrocasts, and 12 of 13 dredge stations were successfully completed. The location of the camera tracks is shown in Figure 5, and the dredge and hydrocast stations in Figure 6.

The camera stations provided about 7300 black and white photographs and 900 in color. The photographs are mostly from the valley floor, and only locally do they show the scarps and terraces bordering the floor (Fig. 5). Sheet flows (Fig. 8A) are the dominant lava morphology on the valley floor, although pillow lavas are observed locally and are common on the valley walls.

About 30 of the black and white photographs show the hydrothermal deposits at the five vent localities (Fig. 5; Fig. 8B,C,D). The color and texture of the deposits are strikingly different from that of pillow and sheet-flow lavas and talus blocks seen in the other 8000+ photographs, so identification of the vent areas is rather straightforward. In addition, the clustering of many worms, mollusks, and stalked(?) organisms seen in the vent photographs is not observed on the lava-flow surfaces elsewhere in the axial valley. The four most prominent vents are located in a depression along the center of the valley (Fig. 7). There is not sufficient photographic evidence at this time to provide accurate outlines or thicknesses of the hydrothermal deposits.

Eleven of the dredge stations recovered fragments of sheet flows, pillow lavas, and other fragments of fresh, glassy basalt. The location of the dredges is given in Figure 6. The twelfth successful station (22) recovered basalt and massive sulfide deposits. This transponder-positioned dredge station was placed over the second vent area discovered during the photographic survey. Several hundred kilograms of basalt and 12 kg of sulfide minerals were recovered. The sulfide deposits are described in detail in part B of this open file report (Koski and others, 1982), and the basaltic rocks are described in part C (Eaby and Clague, 1982).

Two hydrocast stations were positioned above the depression along the axial valley. Station 14 is near the shallowest point along the valley floor, and station 25 is near the vent from which sulfide deposits were recovered (Fig. 6). Analyses still in progress indicate that station 14 was in a plume of hydrothermal water, as there are elevated values of methane, helium-3, and dissolved manganese to at least 150 m above the seafloor. The manganese content at station 14 exceeds background values for the northeast Pacific Ocean by more than two orders of magnitude (J. Murray, personal communication). The final results of the water chemistry measurements will be discussed in a later report.

GEOLOGIC SUMMARY

Geologic features of the rift valley identified from 12-kHz and 3.5-kHz sounding records and from station results are summarized in Figure 7. In the study area, the rift valley and ridge is remarkably symmetric (Fig. 4, profile B-B'). Profiles extending 30 kilometers to either side of the axis still display a high degree of symmetry. The rift valley is about 100 meters deep and the floor averages 1 kilometer in width. The inner valley walls, including a low terrace about 30 meters above the valley floor on most profiles, are formed by steep normal faults. Pillow basalts were photographed and dredged from the inner valley walls, but seem to be less common on the valley floor. Large talus blocks were photographed at the base of scarps forming the valley walls.

About 80-90% of the valley floor consists of low relief, ropy pahoehoe basalt flows (also referred to as sheet flows) (Fig. 8a). In places the flows are strongly striated. A young age is indicated for the basalt by the abundance of fresh glass in the dredge samples and photographs and by the thin sediment cover. The sheet flows take on a more lobate form in places, particularly near the central depression.

The pinger records and photographs indicate that the central depression is bounded by sharp rims. The floor of the depression is much rougher than the floor outside the depression and scattered pillars occur within the depressions. These features suggest that the depression, at least locally, is some type of collapse pit or drainback feature (Ballard and others, 1979; Francheteau and others, 1979).

Four of the hydrothermal vents are in or on the edges of the central depression. Several camera stations which crossed the depression but did not photograph vent animal communities did indicate clusters of benthic siphonophores on the rims and ledges of the depression. The fifth vent is located on a scarp at the base of the eastern wall. This vent site is poorly defined compared to those in the central depression, because it is based only on one clear photograph, which shows a nonvolcanic, unsedimented surface of presumed hydrothermal deposits with possible fragments of worm tubes.

No evidence for hydrothermal circulation was seen between the central depression and the valley walls. This is consistent with the observation that the valley floor contains few fissures and no faults. The only apparent channels for recharge and venting of fluids seem to be along the central depression and the normal faults forming the inner walls.

The hydrothermal vents are characterized by dense concentrations of small worm tubes, larger attached tube and/or stalked creatures, clams, and possibly other types of molluscs (Fig. 8b,c, and d). Two types of hydrothermal deposits are seen in the photographs: (1) bright white hydrothermal precipitate, probably amorphous silica, and (2) dark and light gray encrustations and slabs of massive sulfide minerals, which appear to be similar to the sulfide samples recovered from vent 2 (see Koski and others, part B of this open file).

No hydrothermal vents were photographed in the southern 5 kilometers of the survey area; however, the manganese measurements at hydrocast station 14 suggest that active hydrothermal circulation is occurring there, 1.5 km south of vent 1. The northern extent of the vents is not known, as vent 4 is near the northern limit of the camera stations (Fig. 5).

COMPARISON WITH OTHER RIDGE-CREST HYDROTHERMAL SITES

The hydrothermal vents are located at and to the north of the shallowest point of the southern 35-km segment of the ridge. At 21°N on the East Pacific Rise there is a well defined slope of the rift valley with the highest temperature hydrothermal vents located at the shallowest point (Ballard and others, 1981; Ballard and Francheteau, 1980). A similar along-strike variation in axial depth and venting temperature is suggested at the Galapagos Ridge at 86°W (Ballard and others, 1982; R. D. Ballard, personal communication, 1981). Unlike the Galapagos and 21°N sites, however, the vents at Juan de Fuca Ridge are located in a depression, formed either by faulting and/or lava-lake collapse structures, rather than along a pillow-basalt ridge or a fault-bounded axial block (Law and others, 1981). Ballard and others (1982) suggest a sequence of eruption at Galapagos of extensive sheet flows ending with the formation of a low pillow-basalt ridge along the eruptive fissure. Hydrothermal vents occur along the pillow-basalt ridge. At the southern Juan de Fuca Ridge, the recent voluminous sheet-flow eruptions did not culminate in a major episode of pillow-lava extrusion.

The biological communities at the Juan de Fuca vents have some similarities with those observed at vents on the East Pacific Rise near 21°N, but there are clear differences as well. Worm tubes similar to those seen at 21°N are observed in most vent photographs and have been described from the sulfide deposits (Koski and others, part B of this open file report). The large, red-tipped vestimentiferan worms have not been observed at the Juan de Fuca vents nor have any large clam shells been seen; in contrast, both of these animals are seen in abundance at 21°N on the East Pacific Rise. Our photographic traverses across a typical vent area do not show the same sequence of organisms that constitute the halo of animals commonly seen around vents at 21°N. Additional close-up, color photography will be necessary, therefore, to accurately document the constitution of the faunal communities at the Juan de Fuca hydrothermal vents.

REFERENCES

Ballard, R. D., and Francheteau, J., 1980, Volcanism and tectonics of the East Pacific Rise and their relationship to hydrothermal circulation: EOS, v. 61, p. 992.

Ballard, R. D., Francheteau, J., Juteau, T., Rangin, C., and Normark, W. R., 1981, East Pacific Rise at 21°N: the volcanic, tectonic, and hydrothermal processes of the central axis: Earth and Planetary Science Letters, v. 55, p. 1-10.

Ballard, R. D., Holcomb, R. T., and van Andel, Tj. H., 1979, The Galapagos Rift at 86°W, 3, sheet flows, collapse pits, and lava lakes of the rift valley: Journal of Geophysical Research, v. 84, p. 5407-5422.

Ballard, R. D., Morton, J., and Francheteau, J., 1981, Geology and high temperature hydrothermal circulation of ultra-fast spreading ridge: East Pacific Rise at 20°S: EOS, v. 62, p. 912.

Ballard, R. D., van Andel, Tj. H., and Holcomb, R. T., 1982, The Galapagos Rift at 86°W, 5, variations in volcanism, structure, and hydrothermal activity along a 30-kilometer segment of the rift valley: Journal of Geophysical Research, v. 87, p. 1149-1161.

Corliss, J. B., Dymond, J., Gordon, L. I., Edmond, J. M., von Herzen, R. P., Ballard, R. D., Green, K., Williams, D., Bainbridge, A., Crane, K., and van Andel, Tj. H., 1979, Submarine thermal springs on the Galapagos rift: Science, v. 203, p. 1073-1082.

CYAMEX Scientific Team, 1981, First manned submersible dives on the East Pacific Rise at 21°N (Project RITA): general results: Marine Geophysical Researches, v.4, p. 345-379.

Delaney, J. R., Johnson, H. P., and Karsten, J. L., 1981, The Juan de Fuca Ridge -- hot spot -- propagating rift system: new tectonic, geochemical, and magnetic data: Journal Geophysical Research, v. 86, p. 11747-11750.

Eaby, J. S., and Clague, D. A., 1982, Preliminary description of basalt from the Juan de Fuca Ridge: U.S. Geological Survey Open-File Report 82-200C.

Francheteau, J., Juteau, T., and Rangin, C., 1979, Basaltic pillars in collapsed lava-pools on the deep ocean-floor: Nature, v. 281, p. 209-211.

Galapagos Biology Expedition Participants, 1979, Galapagos '79: Initial Findings of a deep-sea biological quest: Oceanus, v. 22, no. 2, p. 3-10.

Hekinian, R., Fevrier, M., Bischoff, J. L., Picot, P., and Shanks, W. C., 1980, Sulfide deposits from the East Pacific Rise near 21°N: Science, v. 207, p. 1433-1444.

Hekinian, R., Fevrier, M., Needham, H. D., and Avedik, F., 1981, Sulfide deposits: East Pacific Rise near 13°N: EOS, v. 62, p. 913.

Koski, R. A., Goodfellow, R., and Bouse, R. M., 1982, Preliminary description of massive sulfide samples from the Juan de Fuca Ridge: U.S. Geological Survey Open-File Report 82-200B.

Law, S., Malahoff, A., Embley, R., and Fornari, D., 1981, Massive polymetallic sulfides of the Galapagos rift: EOS, v. 62, p. 1027.

Lonsdale, P., 1977, Structural geomorphology of a fast-spreading rise crest: the East Pacific Rise near 3°25'S: Marine Geophysical Researches, v. 3, p. 251-293.

Lonsdale, P., Becker, K., Campbell, A., Elders, W., and Stout, P., 1982, Hydrothermal vents and sulfide deposits at a Gulf of California spreading center: Earth and Planetary Science Letters, in press.

National Ocean Survey, 1974, NOS Seamap Series, North Pacific Ocean, map NOS 12042-12M, scale 1:1,000,000.

Pacific Geoscience Centre, 1978, Juan de Fuca Plate Map: Relief, Map JFP 2, scale 1:2,000,000.

RISE Project Group, 1980, East Pacific Rise: hot springs and geophysical experiments: Science, v. 207, p. 1421-1433.

FIGURE CAPTIONS

Figure 1. Location of mid-ocean ridge segments where active hydrothermal circulation and associated massive sulfide deposits have been observed. Also shown are DSDP sites 504B and 471 (open circles) where similar sulfide mineral deposits have been recovered at depth.

Figure 2. Bathymetry of the Juan de Fuca Ridge and surrounding regions (from Pacific Geoscience Center, Juan de Fuca plate map, 1978). Location of the U.S.G.S. work area during 1980 and 1981 R/V S.P. LEE cruises is shown by the crosshatched box.

Figure 3. Bathymetry of a short segment of the southern Juan de Fuca Ridge based on 12-kHz echo-sounding profiles obtained during the 1980 cruise. Much of the detail on the shape of the axial valley resulted from the 1981 cruise. Hydrothermal vents were identified with bottom photography. The locations of cross sections shown in Figure 4 are indicated.

Figure 4. Bathymetric cross sections through the study area parallel (A-A') and perpendicular (B-B') to the ridge axis. Section A-A' presents changes in depth along strike of the axial valley floor. The hydrocast stations consisted of 6 30-liter Niskin bottles between 1950 m and 2200 m water depth. See Figure 3 for location of profiles.

Figure 5. Location of camera tracks and hydrothermal vents in the rift valley. Arrows indicate the direction of movement of the towed vehicle. Vents 1 and 2 were identified on several crossings, and their known extent is shown with stipled pattern. Vents 3, 4, and 5 were identified on only one camera crossing and are limited to several tens of meters in width along track. The center of the "X" marks the location (and in one case, the extent) of the vent. The acoustic transponder beacons and vent locations are repeated on all maps for local reference points.

Figure 6. Location of dredge and hydrocast stations. Arrows indicate the direction of movement of the dredge. The massive sulfide deposits were recovered at station 22D, and a hydrothermal plume was sampled at station 14H. Vent symbols are the same as in figure 5.

Figure 7. Geologic sketch map of rift valley based on interpretation of 3.5-kHz and 12-kHz records, sled-mounted pinger record, and photographic, dredge, and hydrocast stations.

Figure 8. (a) Low relief, pahoehoe basalt flows with light sediment cover which characterize 80-90% of the axial-valley floor. Ropy to straited surface is common. Highly reflective areas are fresh basaltic glass.

(b,c & d) Representative photographs of hydrothermal vent fields. Rock material consists of dark encrustations and ledges of sulfide minerals, (best shown at upper left in 8c and right side in 8d and bright patches of hydrothermal precipitate, probably amorphous silica shown at lower left in 8c. Dense communities of mollusks and small worm tubes occupy cracks in dark sulfide deposits and locally small worm tubes completely cover underlying sulfide and/or basalt surfaces (8c, center bottom). Larger attached organisms may be a type of tube worm or a stalked creature. Cloudy region in the upper half of 8d could be due to warm, shimmering water. Scale bar in upper right corner of each figure is approximately 1 meter.

figure 1

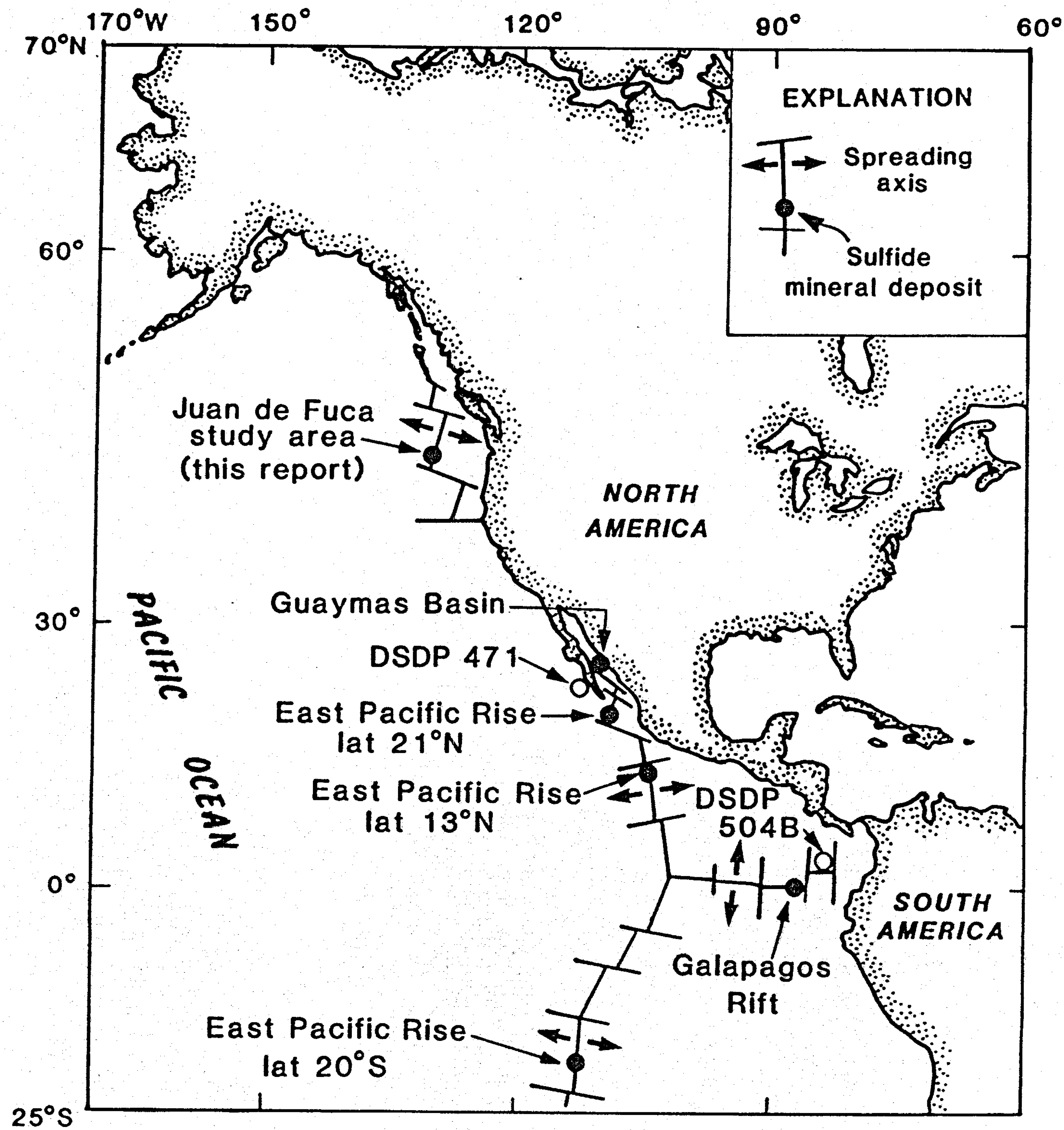
170°W
150°
120°
90°
60°
70°N
60°
30°
0°
25°S
EXPLANATION
Spreading axis
Sulfide mineral deposit
Juan de Fuca study area (this report)
NORTH AMERICA
PACIFIC OCEAN
Guaymas Basin
DSDP 471
East Pacific Rise lat 21°N
East Pacific Rise lat 13°N
DSDP 504B
SOUTH AMERICA
Galapagos Rift
East Pacific Rise lat 20°S

figure 2

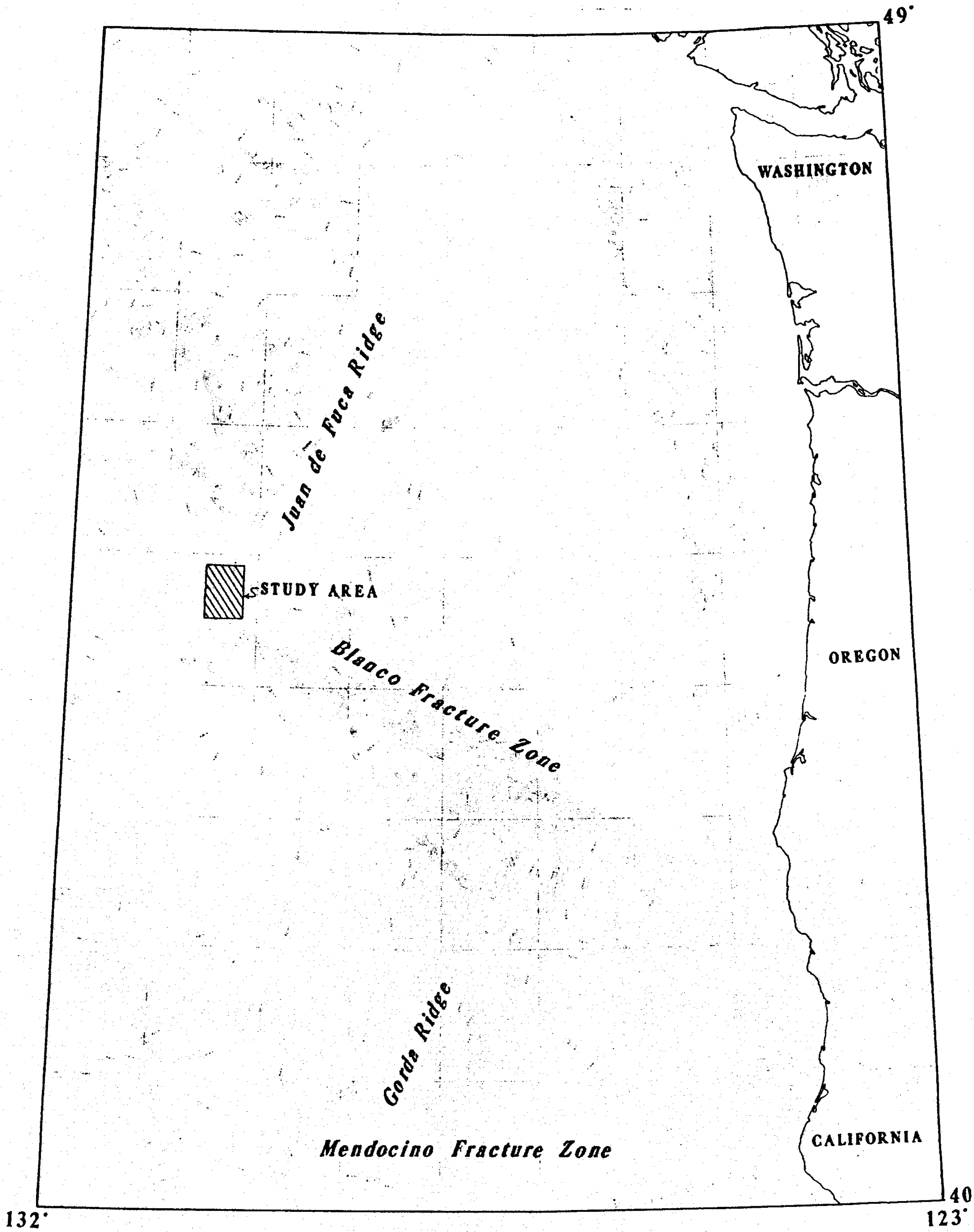
49°
WASHINGTON
Juan de Fuca Ridge
STUDY AREA
Blanco Fracture Zone
OREGON
Gorda Ridge
Mendocino Fracture Zone
CALIFORNIA
40°
132°
123°

figure 3

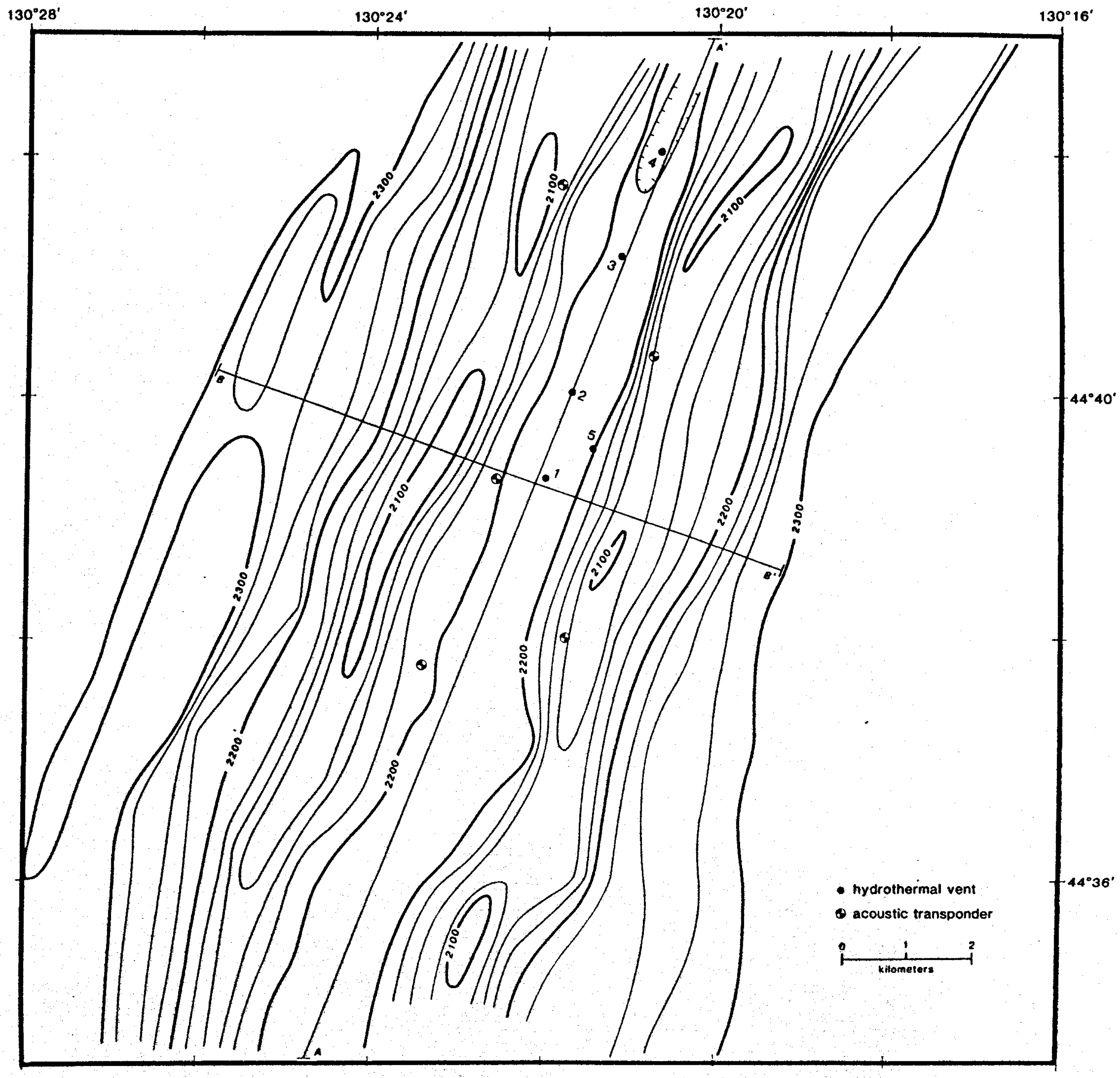
130°28'
130°24'
130°20'
130°16'
44°40'
44°36'
2300
2100
2200
A
A'
B
B'
1
2
3
4
5
hydrothermal vent
acoustic transponder
0
1
2
kilometers

figure 4

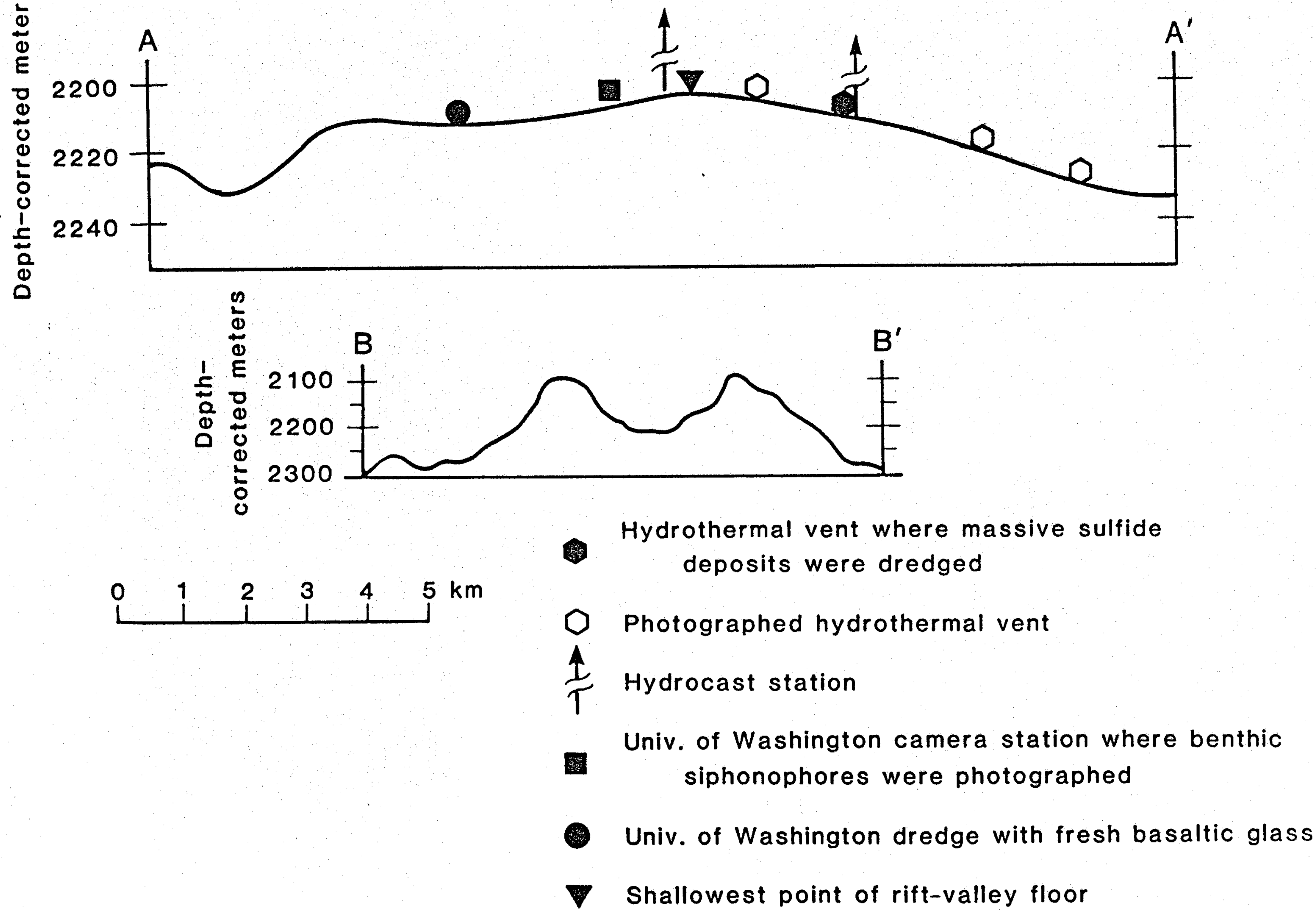
Depth-corrected meters
A
A′
2200
2220
2240
Depth-corrected meters
B
B′
2100
2200
2300
0 1 2 3 4 5 km
Hydrothermal vent where massive sulfide deposits were dredged
Photographed hydrothermal vent
Hydrocast station
Univ. of Washington camera station where benthic siphonophores were photographed
Univ. of Washington dredge with fresh basaltic glass
Shallowest point of rift-valley floor

figure 5

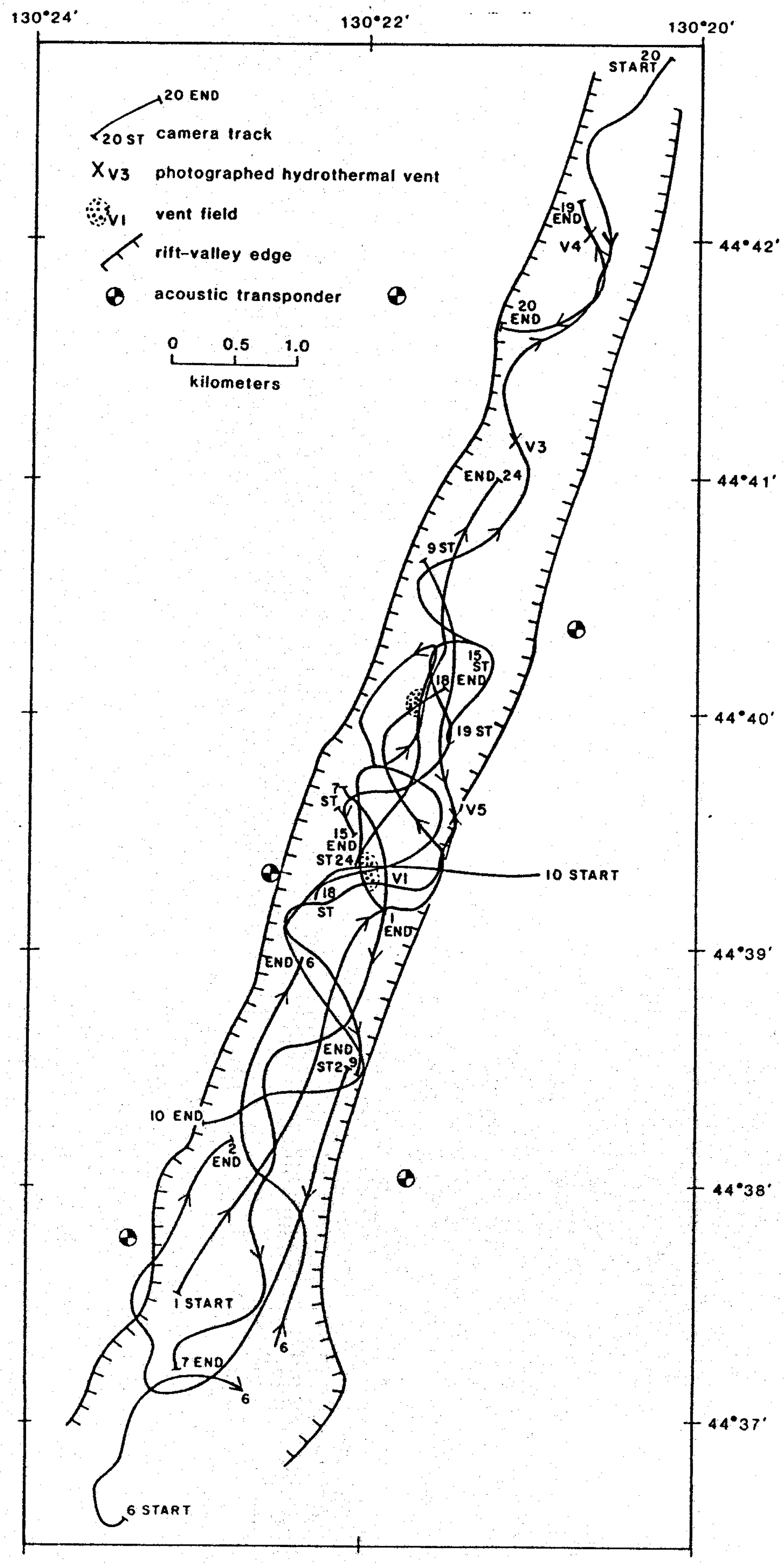
130°24'
130°22'
130°20'
44°42'
44°41'
44°40'
44°39'
44°38'
44°37'
20 END
20 ST
camera track
V3
photographed hydrothermal vent
V1
vent field
rift-valley edge
acoustic transponder
0
0.5
1.0
kilometers
20 START
19 END
V4
20 END
V3
END 24
9 ST
15 ST
18 END
19 ST
7 ST
V5
15 END
ST24
V1
10 START
18 ST
1 END
END 6
END
ST2
9
10 END
2 END
1 START
6
7 END
6
6 START

figure 6

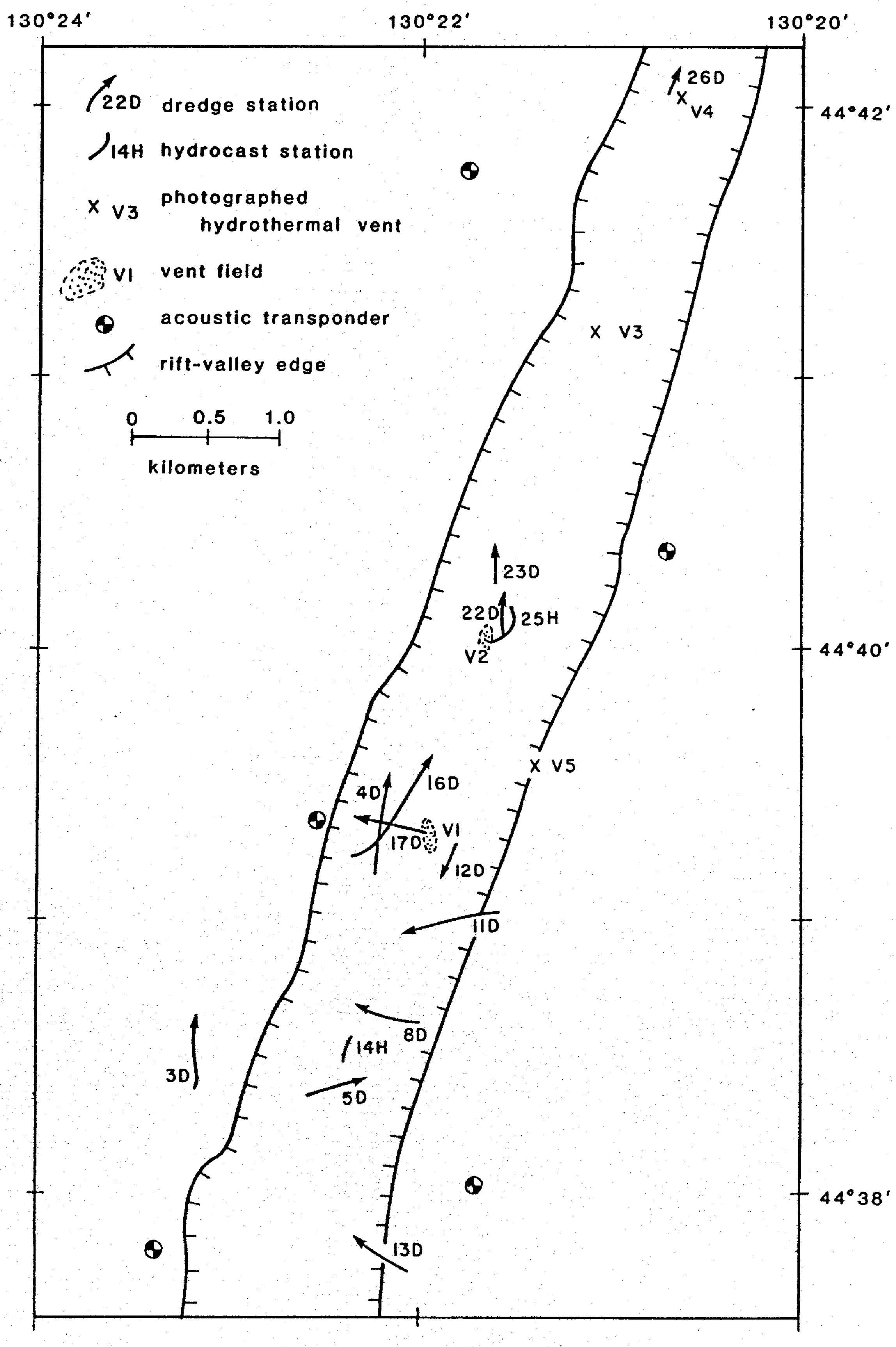

130°24'
130°22'
130°20'
44°42'
44°40'
44°38'
22D dredge station
14H hydrocast station
X V3 photographed hydrothermal vent
VI vent field
acoustic transponder
rift-valley edge
0 0.5 1.0
kilometers
26D
V4
V3
23D
22D
25H
V2
V5
16D
4D
VI
17D
12D
11D
8D
14H
3D
5D
13D

figure 7

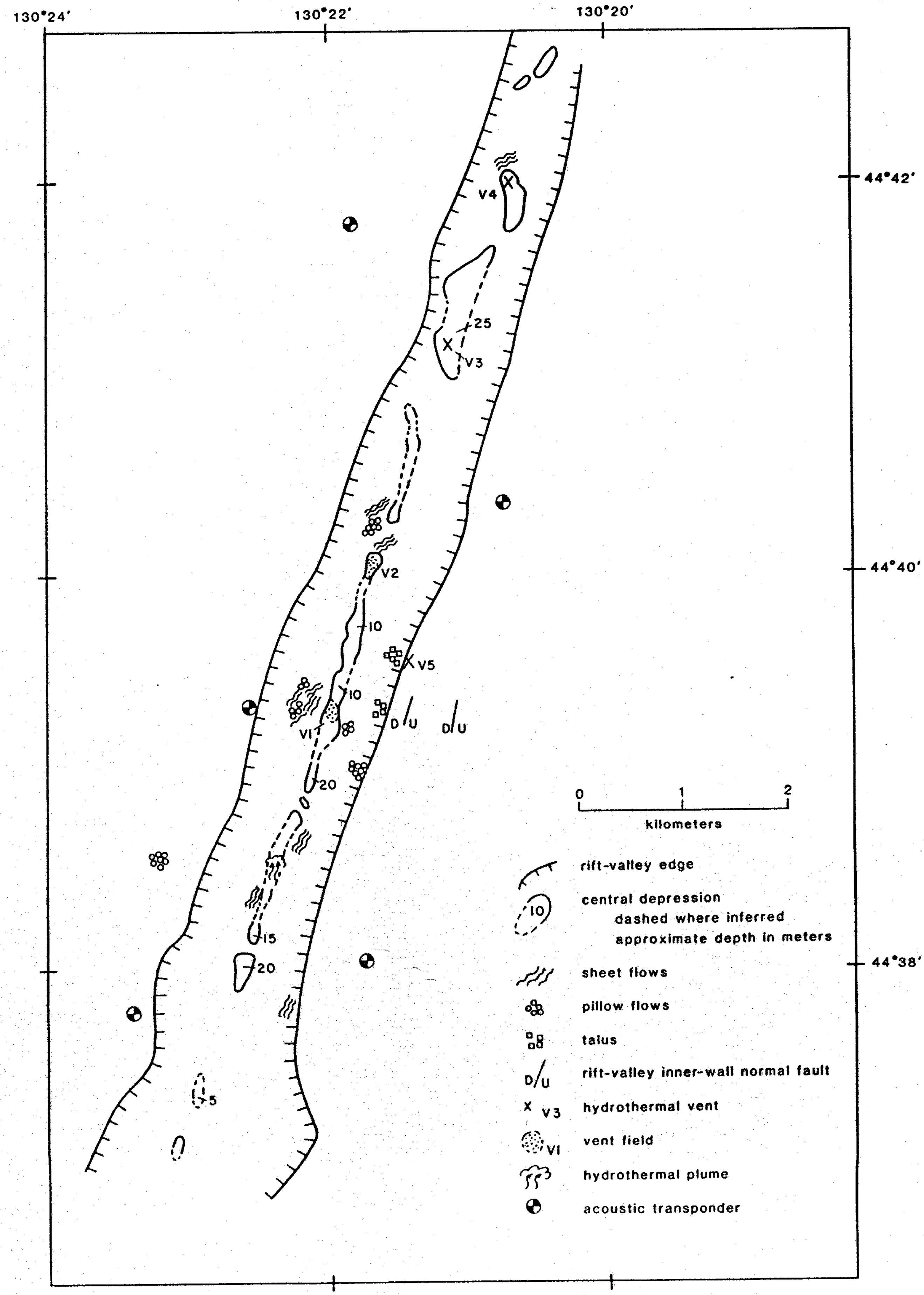

130°24'
130°22'
130°20'
44°42'
44°40'
44°38'
V4
25
V3
V2
10
V5
10
VI
D U
D U
20
15
20
5
0
1
2
kilometers
rift-valley edge
central depression
dashed where inferred
approximate depth in meters
sheet flows
pillow flows
talus
rift-valley inner-wall normal fault
hydrothermal vent
vent field
hydrothermal plume
acoustic transponder